Multiphoton fluorescence microscopic imaging through double-layer turbid tissue media

Xiaoyuan Deng, Xiaosong Gan, and Min Gu[a)]
Centre for Micro-Photonics, School of Biophysical Sciences and Electrical Engineering, Swinburne University of Technology, P.O. Box 218, Hawthorn, Victoria 3122, Australia

(Received 17 September 2001; accepted for publication 11 January 2002)

Image formation in multiphoton fluorescence microscopy through double-layer turbid tissue media is investigated using Monte Carlo simulation. With the help of the concept of the effective point spread function, the relationship of image resolution and signal level to the thickness and scattering properties of the double-layer turbid media under single-, two-, and three-photon excitation is revealed. Results show that for a double-layer turbid medium of a given thickness, small particles in the top layer result in a quicker degradation of signal level than large particles in the top layer. This model is then applied to study the penetration depth of multiphoton fluorescence microscopy through human skin tissue which exhibits a layered structure. It is predicated that using $3p$ excitation leads to a signal level up to two orders of magnitude higher than that under $2p$ excitation, while diffraction-limited image resolution can be maintained for skin tissue of thickness up to 500 μm. © *2002 American Institute of Physics.* [DOI: 10.1063/1.1459107]

I. INTRODUCTION

Two-photon ($2p$) fluorescence microscopy is a useful tool for biological and medical studies[1] because it allows one to achieve an image of a thick sample without using a confocal geometry.[2] Because of the utilization of an infrared laser beam for excitation, this technique offers an equivalent access to ultraviolet (UV) excitation and reduces the effect of Rayleigh scattering in tissue media.[1,3,4] Therefore, this method has been adopted in high-resolution imaging through a thick tissue.[5,6] Since the strength of Rayleigh scattering is inversely proportional to the fourth power of the illumination wavelength, it has been expected that the effect of multiple scattering in tissue media can be further reduced under three-photon ($3p$) excitation.[7,8] However, the effect of Mie scattering on multiphoton excitation is more complicated.[4]

To understand the effect of multiple scattering on image quality (resolution and signal level) in single-photon ($1p$) and two-photon ($2p$) fluorescence microscopy, one usually uses the Monte Carlo simulation method based on Mie scattering and geometric optics[9–11] because conventional image theory[12] based on Fourier optics is not applicable. In particular, the concept of the effective point spread function (EPSF), which describes not only the property of a microscopic imaging system but also the scattering property of turbid media,[13] has been introduced for fluorescence image simulation.[4,9] As a result, the relationship of image resolution and signal level to the focal depth in a turbid medium has been obtained under $1p$ and $2p$ excitation.[4,9]

So far, the turbid media considered in current microscopic Monte Carlo simulations[4,9–11] are single-layer structures. However, biological tissue usually exhibits a complex layer structure such as skin tissue. Although $2p$ and $3p$ fluorescence microscopy has been used to image through skin tissue,[14–17] the penetration depth and the limit of image resolution under multiphoton excitation cannot be determined from the current Monte Carlo simulation model.[4,9–11] This article establishes a Monte Carlo simulation model for $1p$, $2p$, and $3p$ fluorescence microscopic imaging through double-layer turbid media.

This article is organized as follows. In Sec. II, a Monte Carlo model for a double-layer turbid medium is introduced in terms of the concept of the EPSF for multiphoton fluorescence microscopy. The effect of the size of scattering particles and the thickness of a double-layer structure on the EPSF is investigated in Sec. III. Transverse image resolution and signal level through a double-layer turbid medium under $1p$, $2p$, and $3p$ excitation are analyzed in Sec. IV. In Sec. V, the new Monte Carlo model is applied to investigating transverse image resolution and signal level in a skin tissue medium under $1p$, $2p$, and $3p$ excitation. Finally, a conclusions is given in Sec. VI.

II. MONTE CARLO SIMULATION MODEL FOR A DOUBLE-LAYER TURBID MEDIUM

A schematic diagram for imaging through a double-layer turbid medium in a reflection-mode fluorescence microscope is shown in Fig. 1. The top and bottom layers of thicknesses d_1 and d_2 are labeled with L_1 and L_2, respectively. The focal depth f_d is defined as the distance between the medium surface to the focal plane. The Monte Carlo simulation method is similar to that reported elsewhere[9] except for the treatment for the interface between the two layers. When a photon is incident on the interface, a weighting function is given to the reflected and transmitted photons according to the Fresnel coefficient.[18]

Two steps are involved in order to derive an EPSF at a given focal depth f_d. First, a photon distribution $I_{ex}(r)$ (where r is the radial distance from the focus) is calculated

a)Electronic mail: mgu@swin.edu.au

 © 2002 American Institute of Physics

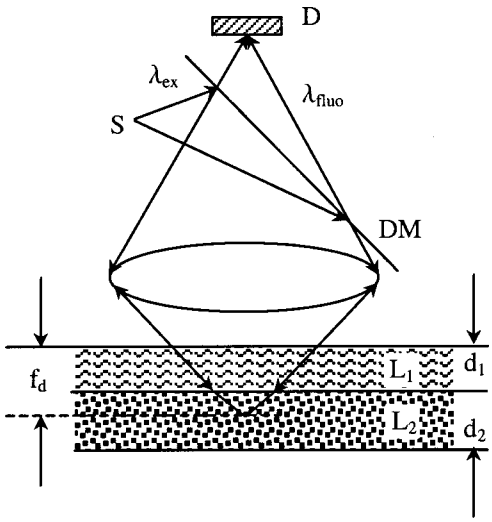

FIG. 1. Schematic diagram of imaging through a double-layer turbid medium in a reflection-mode fluorescence microscope. S: source; D: detector; DM: dichromic mirror; L_1 and L_2: top and bottom layers; d_1 and d_2: the thickness of L_1 and L_2; f_d: the focal depth; λ_{ex} and λ_{fluo}: the wavelength for excitation and fluorescence.

using the Monte Carlo simulation, giving a weighting function for a fluorescence photon.[9] For $1p$, $2p$, and $3p$ excitation, the weighting function can be expressed as

$$p_n(r) = \alpha_n I_{ex}^n(r), \tag{1}$$

where $n=1$, 2, 3 corresponds to $1p$, $2p$, and $3p$ excitation, respectively. In the second step of the Monte Carlo simulation, fluorescence photons excited by Eq. (1) are traced from the positions where they are excited and to the detector plane. Those fluorescence photons reaching the detector lead to a photon distribution $h_n(r)$ which is termed as the EPSF.[9,13] Thus the image intensity of an object with a fluorescence strength function $O(x,y)$ can be given by a convolution relation:[13]

$$I_n(x,y) = \int \int_{-\infty}^{\infty} h_n(\sqrt{x^2+y^2}) O(x-x', y-y') dx' dy'. \tag{2}$$

In the Monte Carlo simulation, 10^7 illumination photons were used to ensure the accuracy of an EPSF under $1p$, $2p$, and $3p$ excitation. The numerical aperture of the objective was chosen to be 0.25 as our previous study has shown that such an objective can remove scattered photons effectively without losing signal appreciably.[9] Furthermore, the effect of refractive index mismatching is negligible for an objective with numerical aperture less than 0.25.[19] It is assumed that the wavelength of the excitation beam, λ_{ex}, under $1p$, $2p$, and $3p$ excitation is 400, 800, and 1200 nm, respectively, and that the fluorescence wavelength λ_{fluo} is 400 nm in the three cases.

To compare the results of a double-layer turbid medium with those from a single-layer turbid medium,[9] we choose two kinds of spherical scattering particles suspended in water. The first kind, called large particles (L), has a diameter ρ of 0.48 μm, and the second one, called small particles (S), has a diameter of 0.202 μm. Each layer in the double-layer structure consists of either large particles or small particles. If the top layer (L_1) includes large particles and the bottom layer (L_2) includes small particles, the double-layer turbid structure is called the LS medium. Otherwise, it is called the SL medium. The thickness of each of the two layers of the media is assumed to be 60 μm. According to Mie scattering theory,[20] the corresponding anisotropy value g and scattering mean free path length l_s are shown in Table I.

III. EFFECTIVE POINT SPREAD FUNCTION IN DOUBLE-LAYER TURBID MEDIA

As EPSF is a performance measure of an imaging system including a turbid medium, the EPSF at different focal depths in the LS and SL media under $1p$, $2p$, and $3p$ excitation is investigated in this section.

The EPSFs for $1p$ fluorescence imaging at three focal depths in the LS and SL scattering media are shown in Figs. 2(a) and 2(b), respectively. The focal depths of 40, 60, and 80 μm mean that the focus is within the top layer, at the boundary, and within the bottom layer, respectively. As expected, when the focal depth increases, the EPSF becomes broader in both LS and SL media because of the increase of the scattering events.[9]

A comparison of the EPSFs between the LS and SL media shows two physical features. First, at a given focal depth (Fig. 3), the EPSF in the LS case is narrower than that in the SL case. Second, the difference of the EPSF between LS and SL media in the bottom layer is smaller than that in the top layer. These properties can be understood from the change in the anisotropy value g in the LS and SL media. According to our previous studies,[21] a smaller scattering particle with a lower anisotropy value g results in a larger scattering angle and thus a broader distribution of scattered photons. Consequently, when the focal depth is moved into the bottom layer, the broadening of the EPSF in the SL medium becomes slower, whereas that in the LS medium becomes quicker, which leads to the behavior in Fig. 3(b).

Figure 4 gives the EPSFs for $2p$ fluorescence imaging at the three focal depths in the LS and SL turbid media. It can be seen that the EPSF in both LS and SL media does not

TABLE I. Scattering parameters of the turbid media under $1p$, $2p$, and $3p$ excitation.

	$1p$ excitation $\lambda_{ex}=400$ nm		$2p$ excitation $\lambda_{ex}=800$ nm		$3p$ excitation $\lambda_{ex}=1200$ nm		Fluorescence $\lambda_{fluo}=400$ nm	
ρ (μm)	g	l_s (μm)	g	l_s (μm)	g	l_s (μm)	g	l_s (μm)
0.48 (L)	0.89	3.68	0.73	15	0.509	44.2	0.89	3.68
0.202 (S)	0.69	3.68	0.2	15	0.086	44.2	0.69	3.68

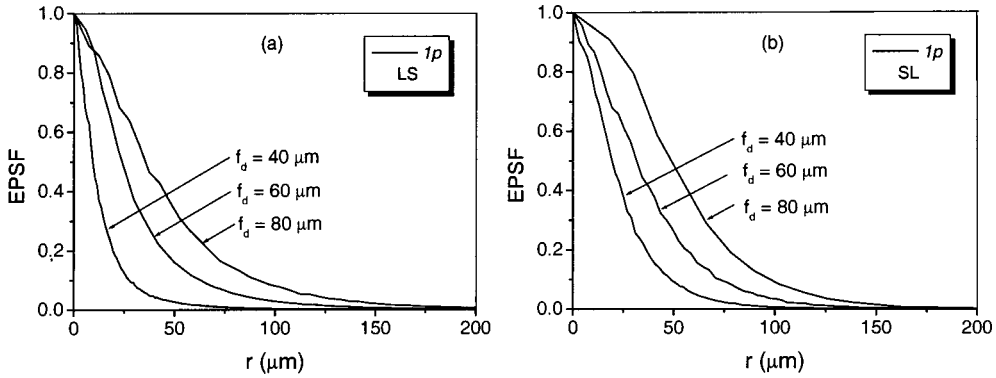

FIG. 2. EPSF for $1p$ fluorescence imaging at different focal depths in the double-layer turbid medium: (a) in the LS medium; (b) in the SL medium.

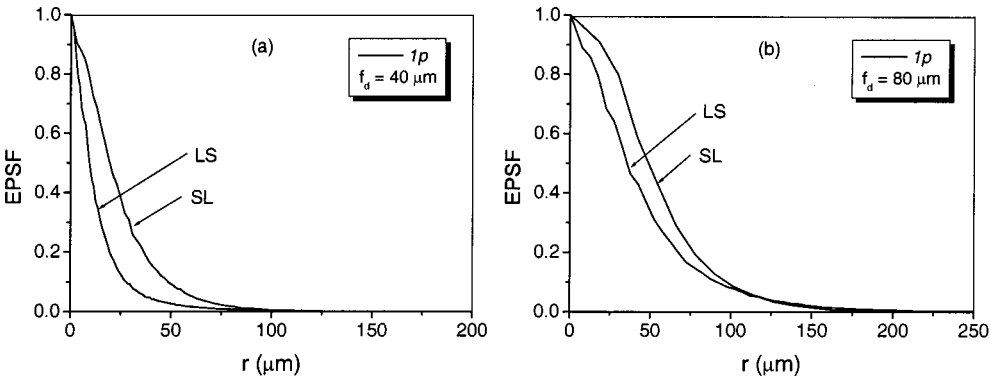

FIG. 3. Comparison of EPSFs for $1p$ fluorescence imaging between LS and SL media. (a) $f_d=40\ \mu$m; (b) $f_d=80\ \mu$m.

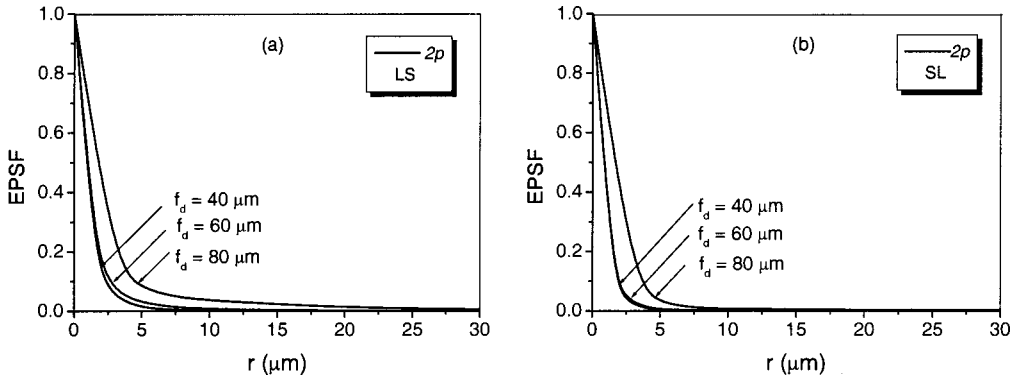

FIG. 4. EPSF for $2p$ fluorescence imaging at different focal depths in the double-layer turbid medium: (a) in the LS medium; (b) in the SL medium.

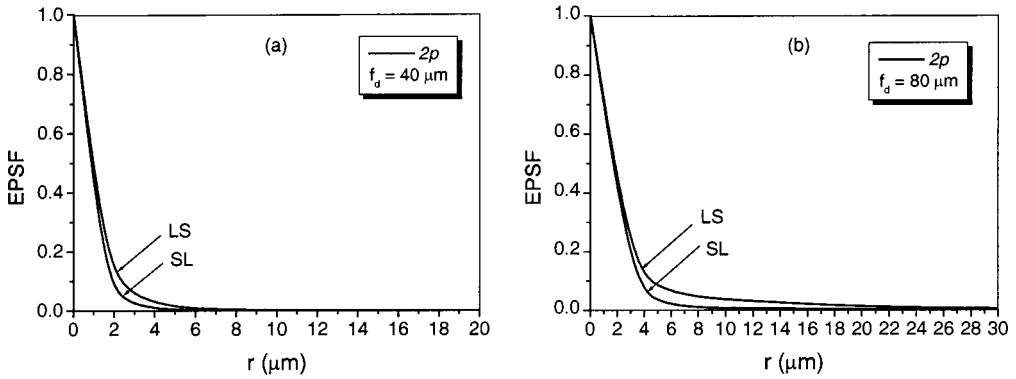

FIG. 5. Comparison of EPSFs for $2p$ fluorescence imaging between LS and SL media: (a) $f_d=40\ \mu$m; (b) $f_d=80\ \mu$m.

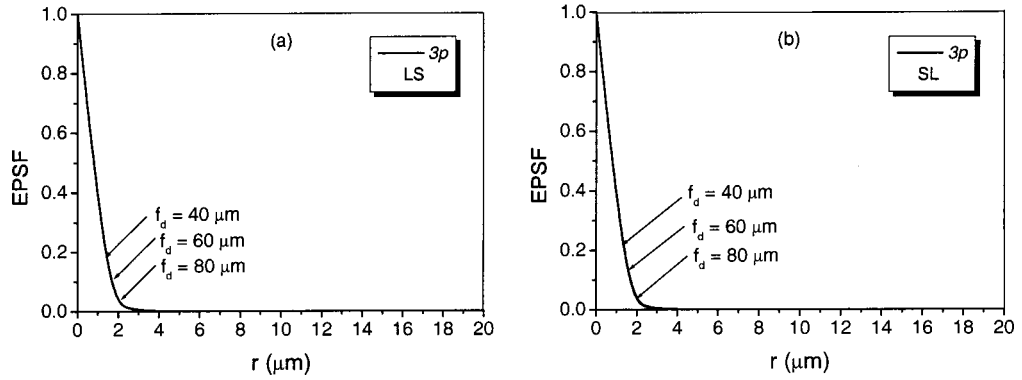

FIG. 6. EPSF for $3p$ fluorescence imaging at different focal depths in the double-layer turbid medium: (a) in the LS medium; (b) in the SL medium.

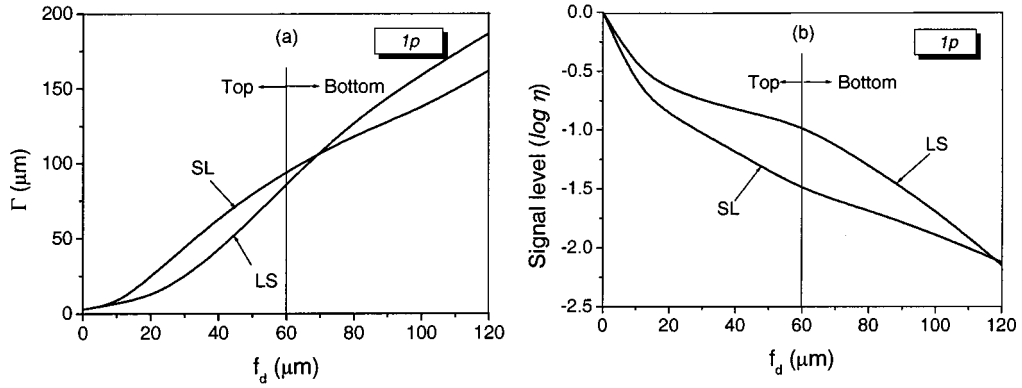

FIG. 7. Transverse image resolution (a) and signal level (b) as a function of the focal depth in the LS and SL media under $1p$ excitation.

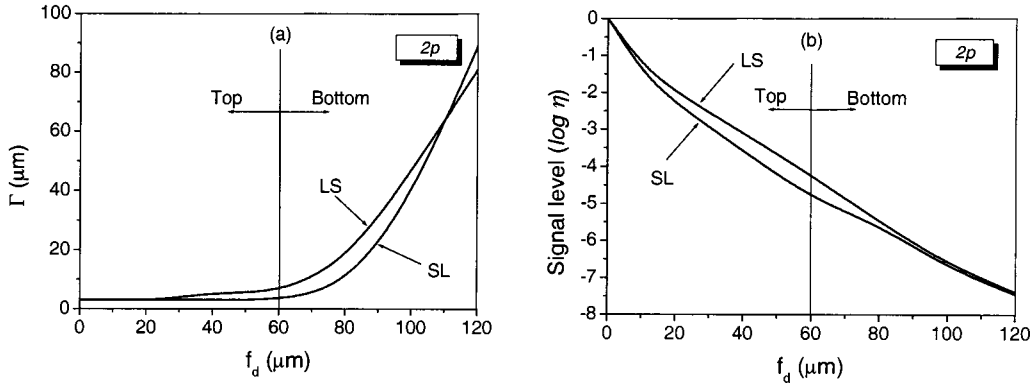

FIG. 8. Transverse image resolution (a) and signal level (b) as a function of the focal depth in the LS and SL media under $2p$ excitation.

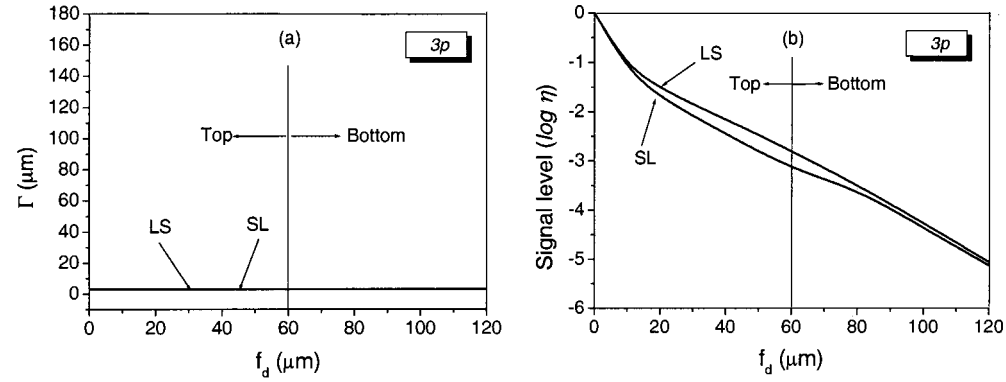

FIG. 9. Transverse image resolution (a) and signal level (b) as a function of the focal depth in the LS and SL media under $3p$ excitation.

change appreciably and that its width is almost close to that predicted by the diffraction theory[12] when the focal depth is less than 60 μm. This feature is caused by the fact that the contribution from ballistic photons to $2p$ fluorescence emission may be dominant when the focal depth is 4–5 times the scattering mean free path length.[9]

Figure 5 shows the comparison of the EPSFs between LS and SL media at a given focal depth. Unlike the situation under $1p$ excitation, the EPSF in the SL medium under $2p$ excitation is slightly narrower than that in the LS medium. This property is consistent with the previous result in the single-layer turbid medium under $2p$ excitation.[9] For the given scattering mean free path length (Table I), the small anisotropy value g in the S layer results in a broad distribution of scattered photons and their contribution to intensity is reduced because of the quadratic intensity dependence under $2p$ excitation. As a result, the central peak mainly resulting from ballistic photons in the SL medium becomes slightly narrower, compared with that in the LS medium.

The EPSFs for $3p$ fluorescence imaging at the three focal depths in the LS and SL media are depicted in Fig. 6. As expected, the EPSF in this case behaves in a diffraction-limited nature because the contribution from ballistic photons is dominant as the given thickness of the double-layer media is only 2–3 times larger than the scattering mean free path length under $3p$ excitation.

IV. TRANSVERSE RESOLUTION AND SIGNAL LEVEL IN DOUBLE-LAYER TURBID MEDIA

Based on the EPSF in the last section, we can investigate image quality in the double-layer turbid medium in terms of image resolution and signal level.[9] The image of a thin sharp edge embedded in a double-layer turbid medium can be calculated using Eq. (2). The transverse image resolution Γ is characterized by the distance between the 90% and 10% intensity points from the image intensity of the sharp edge scanned in the x direction. The signal level η is the number of fluorescence photons collected by the detector and normalized by the fluorescence signal strength when no scattering exists. The advantage of such a definition is that variations caused by the detector sensitivity at different wavelengths and by the excitation cross sections are removed.[4]

The transverse image resolution and the signal level as a function of the focal depth in the LS and SL media under $1p$ excitation are shown in Figs. 7(a) and 7(b), respectively. In general, as the focal depth increases, the transverse resolution becomes poor and the signal level is reduced. Within the top layer, the transverse resolution in the LS medium is better than that in the SL medium. This result is consistent with the behavior of the EPSF shown in Fig. 2 and in our previous study.[9]

To understand the behavior near the interface, we define the rate of resolution degradation, β, as $\beta = d\Gamma/d(f_d)$. Figure 7(a) shows that β below the interface in the SL and LS media is slightly slower and larger than that above the interface, respectively. This feature can be explained by the change in the anisotropy value g in the two layers. In general, photons in the S layer (smaller anisotropy value g) are statistically scattered into a larger angle than those in the L layer (larger anisotropy value g).[21] It was demonstrated[21] that the photons scattered at a larger angle lead to lower resolution than the photons scattered at a smaller angle. As a result, the increase of the anisotropy value g from the S layer to the L layer in the SL medium results in the decrease of β near the interface. In LS medium, the situation is just reserved. This feature implies that the two resolution curves may lead to a cross point at a certain focal depth in the bottom layer, as demonstrated in Fig. 7(a).

In the top layer, the signal level in the LS medium drops more slowly than that in the SL medium, as may be expected from the anisotropy value g in the corresponding layers. The larger the anisotropy value g, the smaller the scattered angle and thus the higher the signal level. Once the focal depth is within the bottom layer, the signal level of the LS medium drops more quickly than that in the SL medium because the anisotropy value g in the bottom layer of the LS and SL media reduces and increases, respectively. As a result, the signal level in the SL medium is lower than that in the LS medium for the given thickness of the media.

Transverse image resolution as a function of the focal depth in the LS and SL media under $2p$ excitation is shown in Fig. 8(a). The transverse resolution in the top layer of the LS and SL media is almost close to the diffraction-limited value, as expected from Fig. 4. Below the interface, the resolution is degraded quickly in both cases, which means that the contribution from scattered photons is significantly increased. The rate of resolution degradation β immediately below the interface is caused by two processes. The first is the change in the anisotropy value g. In terms of the explanation given for Fig. 7(a), this effect leads to the increase and decrease of β from the top to bottom layers of the LS and SL media, respectively. The second process is the significant contribution from the scattered photons when the focal depth is ~ 60 μm,[9] which results in the increase of β in both media. The combination of these two processes gives rise to the fact that the degradation of resolution in the LS medium is faster than that in the SL media when the focal depth moves from the top layer to the bottom layer. Figure 8(b) shows that the change in signal level from the top layer to the bottom layer has the same trend as that under $1p$ excitation.

The dependence of transverse resolution and signal level on the focal depth in the LS and SL media under $3p$ excitation is shown in Fig. 9. Figure 9(a) confirms that the resolution is diffraction limited within the given thickness of the media because of the long scattering mean free path length under $3p$ excitation.

However, the signal level under $3p$ excitation drops quickly although the maximum number of scattering events in the media is less than 3 [see Fig. 9(b)]. It should be pointed out that the number of scattering events is determined by the scattering mean free path length which is a statistically averaged parameter. In other words, even when the number of scattering events is one, i.e., when $f_d = l_s$, $\sim 64\%$ of the incident photons are scattered according to Beer's law. These scattered photons propagate at a large angle from their incident directions because of the small anisotropy value g under $3p$ excitation (see Table I). Conse-

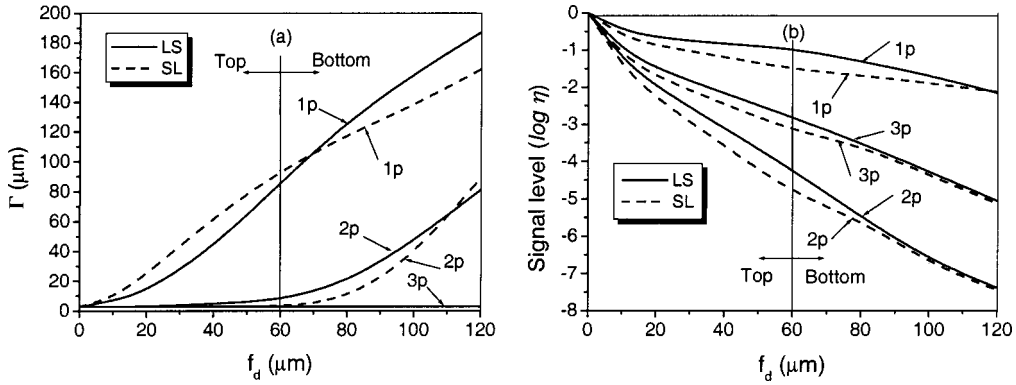

FIG. 10. Comparison of transverse image resolution (a) and signal level (b) in the LS (solid) and SL (dashed) media under $1p$, $2p$, and $3p$ excitation.

quently, the $3p$ fluorescence strength reduces significantly due to the cubic dependence under $3p$ excitation, which leads to the pronounced decay of the signal level. This effect in the S layer is stronger than that in the L layer, so that the signal level in the SL layer is lower than that in the LS layer. It should also be noted that the mean free path length for fluorescence light is significantly shorter than that for excitation wavelength; therefore the scattering effect is strong for the fluorescence light, which results in a further reduction in signal level.

V. DISCUSSION

Compared with the results under $1p$, $2p$, and $3p$ excitation, we can find that in both LS and SL media, $3p$ excitation gives the best transverse resolution [Fig. 10(a)], whereas $1p$ excitation exhibits the worst transverse resolution. Within the top layer, $2p$ and $3p$ excitation leads to the diffraction-limited resolution because of their quadratic or cubic dependence on the excitation intensity and their large scattering mean free path lengths.

A comparison of the signal level under $1p$, $2p$, and $3p$ excitation [Fig. 10(b)] shows two interesting features. First, the signal level in the SL medium is lower than that in the LS medium in all three cases. This feature is because smaller particles (smaller anisotropy value g) in the top layer results in a broader distribution of scattered photons than larger particles (larger anisotropy value g) in the top layer. Accordingly, the reduction of signal in the former case is stronger than that in the latter.

Second, in both LS and SL media the signal level under $3p$ excitation drops more slowly than that under $2p$ excitation but more quickly than that under $1p$ excitation [Fig. 10(b)]. To understand this feature, we take as an example the L layer. In this medium, the ratio of the scattering mean free path length under $3p$ excitation to that under $2p$ is approximately 3. Therefore, the dominant contribution to fluorescence emission under $3p$ excitation is from ballistic photons within the given thickness of the double-layer medium, which leads to a high signal level. On the other hand, because of the smaller anisotropy value g, scattered illumination photons under $3p$ excitation are distributed further away from the geometric focus of the illumination beam than those under $1p$ excitation. This feature together with the cubic dependence of excitation intensity makes the $3p$ fluorescence emission excited by scattered photon less efficient than the $1p$ fluorescence emission, as indicted by Fig. 10(b).

As a demonstration of the significance of the double-layer turbid medium model, we use it to calculate resolution and signal level in human skin tissue under $1p$, $2p$, and $3p$ excitation. Human skin tissue is a complex and highly scattering thick tissue. It can be considered to be a double-layer structure mainly consisting of epidermis and dermis.[14–17] We assume that the wavelength is 365, 730, and 1095 nm for $1p$, $2p$, and $3p$ excitation, respectively, and that the fluorescence wavelength is 450 nm. The absorption and scattering parameters of skin tissue at these wavelengths are summarized in Table II.[22–24] According to the anatomical structure of human skin,[14,22,24] it can be assumed that the thickness of the epidermis and dermis layers is 50 and 450 μm, respectively.

The image resolution Γ and the signal level η of the human skin double layers under three excitation situations are shown in Figs. 11(a) and 11(b), respectively. Because of the big difference of the scattering mean free path length under $1p$ and $2p$ and $3p$ excitation, Γ and η behave differ-

TABLE II. Absorption and scattering parameters of skin tissue under $1p$, $2p$, and $3p$ excitation.

Skin layers	Epidermis			Dermis		
	μ_a (cm^{-1})	g	l_s (μm)	μ_a (cm^{-1})	g	l_s (μm)
$1p$ excitation (λ_{ex}=365 nm)	100	0.72	9.1	7	0.72	21.8
$2p$ excitation (λ_{ex}=730 nm)	39	0.83	23.3	2.4	0.83	55.6
$3p$ excitation (λ_{ex}=1095 nm)	0.87[a]	0.9	84.5[a]	0.87[a]	0.9	84.5[a]
Fluorescence (λ_{fluo}=450 nm)	58	0.75	14.3	4.1	0.75	35.1

[a]Values are from Ref. 24, and others from Ref. 23.

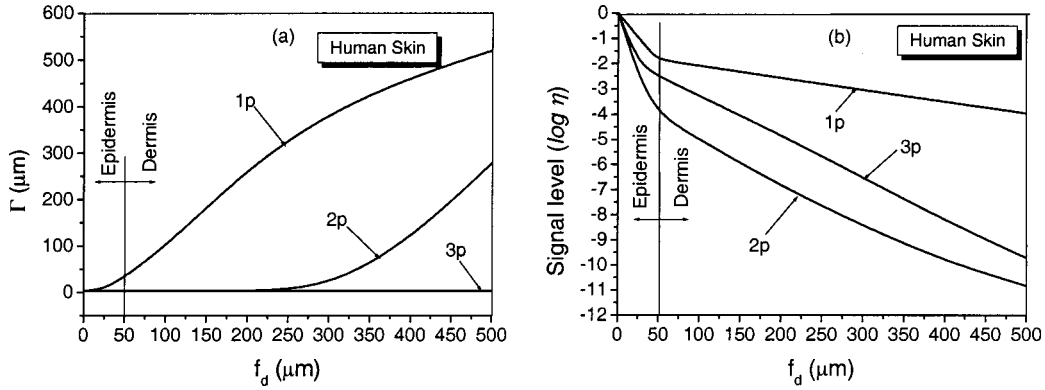

FIG. 11. Comparison of transverse image resolution (a) and signal level (b) in skin tissue under $1p$, $2p$, and $3p$ excitation.

ently. Figure 11(a) shows that the resolution under $3p$ excitation is the best; a diffraction-limited resolution can be kept within the whole thickness of the double-layer skin structure. However, such a diffraction-limited resolution value can be maintained only up to a focal depth of 250 μm (corresponding to a depth of 200 μm in the dermis layer) under $2p$ excitation. Under $1p$ excitation, even within the epidermis layer, the resolution is worse than that of the diffraction-limited value. A comparison of the signal level under $1p$, $2p$, and $3p$ excitation [Fig. 11(b)] shows that the signal level under $3p$ excitation is between those under $1p$ and $2p$ excitation. Within the dermis layer, the $3p$ signal level is approximately 1–2 orders of magnitude higher than that of $2p$ excitation. Consequently, Fig. 11 suggests that $3p$ excitation is a better choice for fluorescence imaging through the human skin tissue than $2p$ excitation.

VI. CONCLUSION

Image resolution and signal level in fluorescence microscopy through double-layer structures under $1p$, $2p$, $3p$ excitation have been investigated using the concept of the effective point spread function produced by Monte Carlo simulation. The dependence of resolution and signal level on the focal depth reveals that the dominant limiting factor under $2p$ and $3p$ excitation is the degradation of signal level. For a double-layer turbid medium consisting of spherical scattering particles, small particles in the top layer result in the quicker degradation of signal level than large particles in the top layer.

It is predicated from our simulation that for human skin tissue of thickness 500 μm, $3p$ excitation gives a diffraction-limited image resolution, while the corresponding signal level is approximately 1–2 orders of magnitude better than that under $2p$ excitation.

It should be indicated that the behavior of EPSF under $1p$ excitation is consistent with that of the absorption distribution[25] in the sense that the effect of scattering is less pronounced if the focal depth is within one mean free path length.

ACKNOWLEDGMENT

The authors thank the Australian Research Council for its support.

[1] W. J. Denk, J. H. Strickler, and W. W. Webb, Science **248**, 73 (1990).
[2] C. J. R. Sheppard and M. Gu, Optik (Stuttgart) **86**, 104 (1990).
[3] V. E. Centonze and J. G. White, Biophys. J. **75**, 2015 (1998).
[4] M. Gu, X. Gan, A. Kisteman, and M. Xu, Appl. Phys. Lett. **77**, 1551 (2000).
[5] Y. Guo, Q. Z. Wang, N. Zhadin, F. Liu, S. Demos, D. Calistru, A. Tirksliunas, A. Katz, Y. Budansky, P. P. Ho, and R. R. Alfano, Appl. Opt. **36**, 968 (1997).
[6] S. P. Schilders and M. Gu, Appl. Opt. **38**, 720 (1999).
[7] S. Hell, S. Bahlmann, M. Schrader, S. Soini, H. Malak, I. Gryczynski, and J. Lakowicz, J. Biomed. Opt. **1**, 71 (1996).
[8] M. Gu, Opt. Lett. **21**, 988 (1996).
[9] X. Gan and M. Gu, J. Appl. Phys. **87**, 3214 (2000).
[10] C. M. Blanca and C. Saloma, Appl. Opt. **37**, 8092 (1998).
[11] A. K. Dunn, V. P. Wallace, M. Coleno, M. W. Berns, and B. Tromberg, Appl. Opt. **39**, 1194 (2000).
[12] M. Gu, *Principles of Three-Dimensional Imaging in Confocal Microscopes* (World Scientific, Singapore, 1996).
[13] X. Gan and M. Gu, Opt. Lett. **24**, 741 (1999).
[14] B. Master, P. So, and E. Gratton, Biophys. J. **72**, 2405 (1997).
[15] P. T. C. So, H. Kim, and I. E. Kochevar, Opt. Express **3**, 339 (1998).
[16] C. Buehler, K. H. Kim, C. Y. Dong, B. R. Masters, and P. T. C. So, IEEE Eng. Med. Biol. Mag. **18**, 23 (1999).
[17] B. Master and P. So, Opt. Express **8**, 2 (2001).
[18] M. Born and W. Wolf, *Principles of Optics* (Pergamon, New York, 1980).
[19] M. Gu, *Advanced Optical Imaging Theory* (Springer, Heidelberg, 2000).
[20] C. F. Bohern and D. R. Huffman, *Absorption and Scattering of Light by Small Particles* (Wiley, New York, 1983).
[21] X. Gan, S. Schilder, and M. Gu, J. Opt. Soc. Am. A **15**, 2052 (1998).
[22] M. J. C. Van Demert, S. L. Jacques, H. J. C. M. Sterenborg, and W. M. Star, IEEE Trans. Biomed. Eng. **36**, 1146 (1989).
[23] V. Tuchin, *Tissue Optics* (SPIE, Bellingham, WA, 2000).
[24] T. L. Troy and S. N. Thennadil, J. Biomed. Opt. **6**, 167 (2001).
[25] L. V. Wang and G. Liang, Appl. Opt. **38**, 4951 (1999).

Journal of Applied Physics is copyrighted by the American Institute of Physics (AIP). Redistribution of journal material is subject to the AIP online journal license and/or AIP copyright. For more information, see http://ojps.aip.org/japo/japcr/jsp
Copyright of Journal of Applied Physics is the property of American Institute of Physics and its content may not be copied or emailed to multiple sites or posted to a listserv without the copyright holder's express written permission. However, users may print, download, or email articles for individual use.